Heliyon 9 (2023) e13709

Contents lists available at ScienceDirect

Heliyon

journal homepage: www.cell.com/heliyon

Research article

Fast and efficient identification of hyaluronidase specific inhibitors from *Chrysanthemum morifolium* Ramat. using UF-LC-MS technique and their anti-inflammation effect in macrophages

Huiji Zhou [a], Xue Zhang [a], Bo Li [a,b,*], Rongcai Yue [c,d,**]

[a] *Amway (Shanghai) Science and Technology Development Co., Ltd, Shanghai, 201203, Shanghai, China*
[b] *Amway (China) Botanical R&D Center, Wuxi, 214145, China*
[c] *School of Pharmacy, Fujian Medical University, Fuzhou, 350122, Fujian, China*
[d] *Fujian Key Laboratory of Drug Target Discovery and Structural and Functional Research, Fujian Medical University, Fuzhou, 350122, Fujian, China*

ARTICLE INFO

Keywords:
Hyaluronidase inhibitors
UF-UPLC-Q-TOF-MS
Chrysanthemum morifolium
Macrophages
Anti-inflammation

ABSTRACT

The purpose of the study was to establish a rapid analytical strategy to screen potential anti-inflammatory compounds from Flos *Chrysanthemum* flower. The enzyme assay was conducted to prescreen botanical extracts, in which *Chrysanthemum morifolium* aqueous extract (CME) displayed hyaluronidase (HAase) inhibitory activity in a dose-dependent manner with the values of 8.31, 24.25, and 66.51% at concentrations of 1.00, 2.00, and 4 0.00 mg/mL, respectively. Eight potential compounds targeting HAase (compounds **9**, **10**, **11**, **13**, **15**, **17**, **20** and **21**) from CME were screened using ultrafiltration affinity liquid chromatography coupled with mass spectrometry (UF-LC-MS) technology. The well-known inhibitor, dipotassium glycyrrhizinate (DG), was used as a positive control and competitive ligand to eliminate false positives. Then, four of these potential components (compounds **9**, **10**, **17,** and **21**), namely eriodictyol-7-*O*-glucoside, luteoloside, apigenin-7-*O*-glucoside and diosmetin-7-*O*-glucoside, were distinguished as potent HAase specific inhibitor candidates with high BD and CBD values. The enzyme inhibitory activities of candidate compounds were verified using enzyme inhibition assay. At a concentration of 1000 μM, compounds **9**, **10**, **17**, and **21** showed 40.15, 44.85, 18.04, and 24.15% inhibition of HAase, respectively. Furthermore, all the four compounds significantly decreased the production of nitric oxide (NO) and IL-6, and significantly suppressed the mRNA expression of inducible NO synthase (iNOS) and IL-1β in both murine and human macrophages.

1. Introduction

Flos Chrysanthemum, known as the flower heads of *C. morifolium* Ramat, is an economically significant food and drug dual-use plant used worldwide [1,2]. It is also one of the most popular flower tea ingredients used in China for the prevention of inflammation and for liver protection [3–5]. In addition, it also commonly used in functional food and beverages and plays a significant role as traditional Chinese medicine for clearing heat, removing toxin, treating fatty liver and improving vision [6,7]. Interestingly, Flos

* Corresponding author. Amway (Shanghai) Science and Technology Development Co., Ltd, Shanghai, 201203, Shanghai, China.
** Corresponding author. School of Pharmacy, Fujian Medical University, Fuzhou, 350122, Fujian, China.
E-mail addresses: robert.li@amway.com (B. Li), yrcowen@163.com (R. Yue).

https://doi.org/10.1016/j.heliyon.2023.e13709
Received 10 November 2022; Received in revised form 5 February 2023; Accepted 8 February 2023
Available online 14 February 2023

Chrysanthemum is primarily consumed in the form of hot-water infusions of the flowers [8]. Several modern pharmacological studies have revealed its antioxidant [9], anti-inflammatory [10], and antiallergic [11] properties. Previous phytochemical studies have illustrated that the main components of Flos *Chrysanthemum* are flavonoids and dicoffeoylquinic acid [12], such as apigenin, luteolin, luteoloside, 1,3-dicaffeoylquinic acid, and 3,4-dicaffeoylquinic acid.

Hyaluronic acid (HA) is a linear acidic mucopolysaccharide that widely exists in skin, joints and soft connective tissues within the body, and is thought to participate in numerous physiological processes, such as inflammation, cell migration, and tumour development [13]. The repeated disaccharide structure of HA was confirmed to be associated with the features of pathogen molecular patterns [14]. It was reported that small HA fragments increase macrophage generation of the cytokines IL-1β and TNF-α, as well as their allostimulatory capacity [15]. Hyaluronidase (HAase) is an endoglycosidase enzyme that plays an important role in HA metabolism [16]. Enzymatic degradation of HA generates a wide range of bioactive oligosaccharides that are attributed for pro-inflammatory, angiogenic, and immunostimulatory properties [17,18]. HAase catalyzes the hydrolysis of HA, leading to breakdown of HA into oligosaccharide fragments, which then trigger the infiltration of exogenous inflammatory mediators into the body and ultimately cause a cascade of inflammatory responses. In the process of inflammation, the content of HAase increases significantly, which further exacerbates the development of inflammation. Previous studies indicated that effective HAase inhibitors may deter HA fragmentation that promotes inflammation, and may therefore exhibit anti-inflammatory properties [19]. Recently, several studies have illustrated the positive findings of plant extractions on inhibiting human HAase [20]. Aqueous extract of *Plantago* and its major compound, calceorioside B, has been reported to display striking inhibition against HAase [21]. *Ravenala madagascariensis* extract was reported to exhibit great HAase inhibition activity, and two promising HAase-combining compounds, epiafzelechin and epicatechin, were isolated using bioassay-guided purification [22].

Ultrafiltration affinity liquid chromatography coupled with mass spectrometry (UF-LC-MS), based on a ligand fishing technique and MS that can identify the target molecules liberated from the enzyme, is frequently used to screen potential bioactive enzyme inhibitors (for example, α-amylase, xanthine oxidase, neuraminidase, and cyclooxygenases) from complex or combinational mixtures, such as herbal extracts, without repetitious and complicated isolation and purification processes [23,24]. Briefly, in this process, ligand-enzyme complexes are separated from herbal mixtures using a bio-affinity UF process, and the ligands that bind to the enzymes are then further identified using LC-MS analysis [24]. However, a major problem in this method is the false positive results induced by non-specific ligand binding [25]. To eliminate false positives, a competitive binding experiment in UF-HPLC was introduced by Chen et al. [26], and has been extensively applied to distinguish selective and specific enzyme inhibitors from natural product matrix [27,28]. Therefore, the UF-LC-MS technique was modified by introducing a competitive blocker as a control to distinguish specific and non-specific ligand binding [29]. However, to the best of our knowledge, the UF-LC-MS method has not been previously used to screen and identify HAase inhibitors from complex mixtures; therefore, developing this method is a current challenge.

In our present study, an approach of UF-LC-MS combined with a competitive binding experiment was tentatively developed to identify compounds from Flos *Chrysanthemum* that potentially affects HAase inhibitory activity and reduces the possibilities of false positives. The limitations of the study were also discussed. As a result, four flavonoids were ultimately identified as potential specific ligands that bind to HAase active sites. Furthermore, their anti-inflammatory effects on the lipopolysaccharide(LPS)-induced inflammatory cytokines and inflammatory mediators in macrophages were analyzed to comprehensively study the anti-inflammatory actions of the four ligands. This study, to the best of our knowledge, is the first to use UF-LC-MS technology to promptly screen and verify HAase inhibitors in Flos *Chrysanthemum* extract (CME), which will further explores possible mechanisms against inflammation for its use as a food and drug dual-use plant, and may offer an efficient method for rapidly identifying bioactive substances as HAase inhibitors from complex products.

2. Materials and methods

2.1. Reagents and materials

Acetonitrile and formic acid (HPLC grade) were purchased from Merck (Darmstadt, Germany). The reference standards dipotassium glycyrrhizinate (DG), Luteolin-7-*O*-glucuronide (>99.0%), 4,5-dicaffeoylquinic acid (>99.5%), 3,5-dicaffeoylquinic acid (>99.0%), 3,4-dicaffeoylquinic acid (>99.5%), luteoloside (>99.5%), eriodoctyol-7-*O*-glucoside (>99.5%), apigenin-7-*O*-glucoside (>99.0%), and diosmetin-7-*O*-glucoside (>99.0%) were purchased from Nature Standard Biotech Co. (China). The RAW264.7 cell line was supplied by the Cell Bank of the Chinese Academy of Sciences (Shanghai, China). High-glucose Dulbecco's modified Eagle's medium (DMEM), foetal bovine serum (FBS) and penicillin-streptomycin stock solution were purchased from Gibco (Carlsbad, CA, USA). LPS from *Salmonella enterica* serotype typhimurium, dimethyl sulfoxide (DMSO), and bovine testicular HAase were purchased from Sigma-Aldrich Chemical Co., Ltd. (St. Louis, MO, USA). The enzyme-linked immunosorbent assay (ELISA) kit for determinations of IL-6 was purchased from Thermo Fisher (Waltham, Massachusetts, USA). The 3-(4,5-dimethylthiazol-2-yl)-2,5-diphenyltetrazolium bromide (MTT) and nitric oxide (NO) kits were purchased from the Jiancheng Bioengineering Institute (Nangjing, China). All chemicals were of analytical grade and used without further purification. Ultrapure water was provided by a Milli-Q laboratory water purification system (Bedford, MA, USA).

2.2. Plant material

The flowering heads of *C. morifolium* were purchased from Lanxi County (Zhejiang, China) in November 2019 and dried in the sun after steaming. It was authenticated as *C. morifolium Ramat.* Flower by doctor Gangqiang Dong, Amway Botanic Research Centre,

China.

2.3. Preparation of the CME

The dried flower sample was milled and sieved through a NO.3 sieve. Twenty grams of powder was accurately weighed and followed using a water reflux extraction (Flos powder: deionized water, 1:12; 100 °C; 60 min/30 min, repeated), filtered and combined. Then the consolidated extract was evaporated to a syrup at 50 °C using a vacuum. Finally, CME was obtained using a vacuum freeze-drying process. The lyophilized extract was then dissolved in distilled water and filtered through a 0.45 μm porous membrane before use.

2.4. Protocol of screening for potential selective HAase inhibitors with UF

The proposed strategy was performed using three steps: co-incubation, UF, and LC-MS identification. CME solution (50 μL, at a final concentration of 10 mg/mL) and 250 μL of HAase solution (at a final concentration of 10 mg/mL HAase in 0.1 M, pH 5.6 acetate buffer) were mixed and co-incubated at 37 °C for 30 min. Subsequently, the unbound ligands were filtered through a Amicon Ultra-0.5 Centrifugal Filter Unit with a 30 kDa MW cut-off membrane (Millipore, Bedford, MA, US) at 15,000 rpm for 10 min at room temperature and washed twice with 300 μL buffer solution. The filtrate was subject to the ultra-high performance liquid chromatography-mass spectrometry (UPLC-MS) analysis. The blank sample was prepared without HAase. Blocked HAase solution was prepared by mixing DG (50 μL, 1 mg/mL) and HAase (250 μL, 10 mg/mL in acetate buffer), and pre-incubated at 37 °C for 30 min, and filtering through a Microcon ultra-centrifugal filter unit with a 30 kDa cut-off membrane through centrifugation at 15,000 rpm for 10 min. The residue was washed with 300 μL buffer solution and centrifugated. Then, the blocked HAase solution was prepared by adding 250 μL acetate buffer for the competitive control experiment with the same procedures. Finally, the eluted solution was stored at 4 °C until further analysis.

The binding capacities of constituents to HAase were determined by comparing the decreased peak area in UPLC chromatograms. The relative binding affinities of the constituents toward HAase were defined as the binding degree (BD), which was calculated using Eq. (1):

$$BD = \frac{A_a - A_b}{A_a} \times 100\% \tag{1}$$

where Aa represented the total ion chromatogram (TIC) peak area of a compound interacting without enzyme, and A_b was the TIC peak aera of the same compound after interacting with active HAase. The HAase competitive binding ability between selected blocker and ligands was defined as the competitive binding degree (CBD), which was determined using the following formula (2):

$$CBD\% = \frac{A_c - A_b}{A_a} \times 100\% \tag{2}$$

where Ac is the TIC peak area of a compound co-incubating with HAase blocked using a known ligand.

2.5. UPLC- quadrupole-time-of-flight tandem mass spectrometry (Q-TOF MS/MS) analysis

The UPLC analysis was accomplished using a Waters UPLC analyser with an Acquity T3 reverse phase column (2.1 × 100 mm, 1.8 μm; Waters) and the UPLC conditions were as follows: mobile phase 0.5% formic acid aqueous solution (A) and acetonitrile (B) with a gradient elution of 10–16% B at 0–4 min, 16–18% B at 4–6 min, 18–20% B at 6–12 min, 20–30% B at 12–20 min, 30% B at 20–25 min; flow rate 0.2 mL·min-1; injection volume, 2 μL; detection wavelength, 348 nm; column temperature, 25 °C. The LC-MS detection was performed using a AB Sciex Triple TOF® 4600 mass system (SCIEX, USA) equipped with an electrospray ionization (ESI) source and operated in negative ion mode. The MS parameters were set as follows: TOF mass range, 100–1500 *m/z*; ion source gas, 50 psi; curtain gas, 35 psi; ion spray voltage, 4500 kV; ion source temperature, 500 °C; and collision energy, 10 eV. The MS/MS parameters were set as follows: MS/MS mass range, 50–1250; collision energy, 40 eV; declustering potential, 100 V; and collision Energy Spread, 20eV.

2.6. HAase inhibition assay

The HAase inhibitory activity of CME and its components was determined by measuring the amounts of *N*-acetylglucosamine released from sodium hyaluronate, using a slightly modified method disclosed previously in literature [30]. Bovine HAase (20 μL, 1 mg/mL in 0.2 M acetate buffer) and 50 μL of test samples dissolved in 10% DMSO were mixed and incubated in a water bathat 37 °C for 20 min. Calcium chloride (10 μL, 2.5 M) was then added and incubated for another 20 min at 37 °C. Sodium hyaluronate (50 μL, 0.5 mg/mL) was then added to the reaction mixture and further incubated for 40 min at 37 °C. After incubation, 50 μL distilled water, 10 μL 5 M NaOH, and 50 μL acetylacetone solution (0.7 mL acetone was dissolved in 10 mL 1 mol/L sodium carbonate solution before use) were added and incubated for 15 min in a boiling water bath. After cooling to room temperature, 100 μL *p*-dimethylaminobenzaldehyde solution (0.08 g *p*-dimethylaminobenzaldehyde was added to 1.5 mL concentrated hydrochloric acid and 1.5 mL absolute ethyl alcohol mixed solution) was added and mixed adequately. Then 400 μL absolute ethyl alcohol solution was added and finally incubated for another 30 min at room temperature. Absorbance was measured at 530 nm. DG was used as a positive control. All

samples were tested in triplicate. The inhibitory activity was calculated using the following formula:

$$\text{Inhibition}\% = [1\text{-}(A1\text{-}A2)/(A3\text{-}A4)] \times 100\%$$

where A1 is the absorbance of both test samples and HAase existence, A2 is the absorbance of the test samples and HAase absence, A3 is the absorbance of the enzyme without the test sample, and A4 is the absorbance using buffer solution instead of test samples and HAase.

2.7. Cell culture assay of cell viability

The murine macrophages RAW264.7 cell line was purchased from Shanghai Institute of Cell Biology, Chinese Academy of Sciences. Cells were cultured in high-glucose DMEM containing 10% FBS, 100 U/mL penicillin, and 100 g/mL of streptomycin at 37 °C in a 5% CO_2 humidified incubator. Cells (5×10^4/mL) were seeded in 96-well plates and incubated overnight, then treated with different concentrations of specific compounds for 2 h. Treated cells were then co-cultured with the addition of LPS (final concentration of 50 ng/mL) for an additional 24 h. The cells cultured in the medium with LPS or without LPS were used as the positive and negative controls, respectively. After incubation, cell viability was measured using a MTT assay kit. The medium was removed, and 50 μL of MTT solution was added to each well and incubated at 37 °C for 4 h. After discarding the supernatants, the crystallized MTT was immediately dissolved in DMSO with sufficient mixing. The absorbance (Abs) was measured at a wavelength of 570 nm. Cell viability rate was evaluated according to the formula below:

Cell viability rate (%) = (Abs 570 of treated cells/Abs 570 of untreated cells) × 100%.

2.8. Assay of NO and determinations of TNF-α and IL-6

Cells (5×10^5/well) were seeded in 24-well plates, incubated overnight and pretreated with 12.5–50 mM of compounds for 2 h prior to 24 h of treatment with 50 ng/mL LPS. Dexamethasone (DXM, 10 μM) was used as positive control. All the cell culture medium was collected and then centrifuged at 4 °C. The cell-free supernatants were harvested for the quantification of NO and inflammatory cytokines, including TNF-α and IL-6. The NO contents in the culture medium was measured using the Griess assay kit. In addition, the levels of pro-inflammatory cytokines TNF-α and IL-6 in the supernatant were quantified using commercial mouse immunoassay ELISA kits according to the manufacturer's instructions.

2.9. Real-time reverse transcription quantitative polymerase chain reaction (RT-qPCR) analysis

Cells (1×10^6/well) were inoculated into 6-well plates and incubated for 24 h, then treated with different concentrations of compounds (12.5, 25 and 50 μg/mL) containing LPS (50 ng/mL) for 4 h at 37 °C. Total RNA was extracted in an RNase-free environment and quantified using the RNeasy Mini Kit (Tiangen, Beijing, China). cDNA was synthesized from 1 μg RNA using the High-Capacity cDNA Reverse Transcription Kit (Thermofisher 4,368,813, Beijing, China) according to the procedures described. Then, RT-qPCR was performed with the PowerUp™ SYBR™ Green Master Mix (Thermofisher A25742, Beijing, China). The cDNA was amplified through 40 cycles of denaturing at 95 °C for 15 s, then annealing and extending at 60 °C for 60 s. The PCR primers (Sangon Biotech, Shanghai, China) used are listed in Table 1. The relative mRNA expression was calculated using the $2^{-\Delta\Delta Ct}$ method. Ct values of GADPH were used as a control for normalization. All reactions were performed in triplicate.

2.10. Human macrophages culture and stimulation

The L929 cell line was purchased from Cellcook, and the THP-1 cell line was purchased from the Stem Cell Bank, Chinese Academy of Sciences. L929 and THP-1 cells were grown in complete DMEM (Hyclone) and Roswell Park Memorial Institute (RPMI) 1640 medium (Hyclone), respectively. Each medium was supplemented with 10% FBS(Gibco) and 1% penicillin-streptomycin (P/S, GA3502, GENVIEW). All cells were maintained at 37 °C with 5% CO_2. THP-1 cells were inoculated into 24-well or 6-well plates overnight and then treated with 100 nM phorbol ester for 3 h. Then THP-1 cells were pretreated with 12.5–50 mM of compounds for 2 h prior to 24 h of treatment with 50 ng/mL LPS. The supernatants and cell lysates were collected for ELISA and qPCR assays.

Table 1
The primer sequences of genes investigated using RT-qPCR analysis.

Gene	Direction	Sequence (5′-3′)
GAPDH	F	AGGTCGGTGTGAACGGATTTG
	R	TGTAGACCATGTAGTTGAGGTCA
IL-1β	F	GGGATGATGATGATAACCTG
	R	TTCGTCGTTGCTTGGTTCTCCT
iNOS	F	GGATCCAGTGGTCCAACCTG
	R	GTTGCCATTGTTGGTGGCAT
MyD88	F	FAGGACAAACGCCGGAACTTTT
	R	GCCGATAGTCTGTCTGTTCTAGT

F: Forward; R: Reverse.

Dexamethasone (DXM, 10 μM) was used as positive control.

2.11. Statistical analysis

The data was statistically processed using Graphpad software. The test data were expressed as mean ± standard deviation (SD), and the results were statistically evaluated using one-way analysis of variance (ANOVA) followed by the Dunnett's test. Statistical significance was set at $*P < 0.05$ and $**P < 0.01$.

3. Results and discussion

3.1. HAase inhibitory activities of CME

HAase is a HA-splitting enzyme that ubiquitously distributes to the extracellular matrix, particularly in soft connective tissue, and plays an important role in maintaining normal penetration ability of tissue membrane and blood vessels, specifically [31]. Consequently, HAase inhibitors have become increasingly vital in the development of new anti-inflammatory drugs from natural products [32,33]. In this study, *C. morifolium*, a well-known and constantly validated anti-inflammatory herb used commonly in China [34], was used to assess the inhibitory effects on HAase. As shown in Table 2, CME displayed HAase inhibitory activity in a dose dependent manner with the values of 8.31, 24.25, and 66.51% at a concentration of 1.00–4 0.00 mg/mL.

3.2. Optimization of HAase incubation conditions

Several recent studies have reported the application of affinity-based UF-HPLC to screen and identify ligands from complex natural mixtures [35–37]. Inspired by previous findings, the aim of the study was to set up an UF-LC screening strategy that can be used to identify specific HAase ligands from CME.

DG, a common HAase inhibitor, has been frequently used as an anti-inflammatory agent [38]. DG inhibits HAase is involved in various inflammatory pathways, and it is often used as positive control for the HAase inhibition assay [39]. In our assay, DG as a proven HAase blocker, was used as a competitor ligand to differentiate specific and non-specific binding, which may minimize the occurrence of false positives. Thus, different UF parameters, including HAase concentrations, incubation times, and incubation temperatures were optimized to increase total binding affinity and eliminate background interference. First, as the concentration of target enzyme is a key influencing factor, DG was incubated with 1, 5, and 10 mg/mL HAase. After separation through centrifugal filters, the ultrafiltrates were analyzed using UPLC. Fig. 1A displays the binding differences of DG with different concentrations of HAase. The peak area of DG decreased with ascending of the enzyme concentration. The largest peak area reduction of DG presented with 10 mg/mL HAase. With insufficient HAase during incubation, competitions among ligands are more likely to occur, which directly affects binding affinity, and leads to potential inhibitors being overlooked [4]. To ensure efficiency, further incubation conditions were all designed at 10 mg/mL HAase.

Incubation temperature is another pivotal factor for the binding rate of HAase. If the temperature is too low, the activity of HAase will be suppressed, whereas temperatures that are too high result in the destruction of enzyme structure or binding-site conversions. The DG was incubated with HAase at 30.0, 37.5, and 50.0 °C to elucidate the appropriate incubation temperature. With the decline of incubation temperature, the peak area of DG increased gradually, indicating the enzyme activity decreased as temperature falls (Fig. 1B). However, at 50 °C, clear precipitation of HAase was observed, which may block membrane pores during centrifugation filtration. Therefore, 37.5 °C was the optimal temperature condition found in the present study.

Incubation time has significant influence on the binding rate of ligands to enzymes. Incubation times that are too short leads to inadequate interaction, and times that are too long decrease screening efficiency. The effect of incubation time on HAase is illustrated in Fig. 1C. The peak area of DG decreased slightly with increased incubation times. Considering these results, 30 min of incubation time was finally selected.

3.3. Screening of HAase inhibition ligands from CME using UF-LC-PDA-MS

UF combined QTOF-MS/MS has been widely applied as a pharmacological profiling tool to identify enzyme inhibitors from complex extracts [40]. This affinity-based approach plays important roles in enzyme targeting-active candidates discovering and identification. The technological process of UF-LC-MS screening is shown in Fig. 2: first, some botanic extract was co-incubated with

Table 2
Inhibitory effects of CME on HAase activity.

	HAase inhibition (% control)		
	1 mg/mL	2 mg/mL	4 mg/mL
Flos Chrysanthemum	8.31 ± 6.05	24.25 ± 5.32[a]	66.51 ± 7.17[a]

All data were expressed as mean ± SD and the negative control value was approximately 0% inhibition of HAase without samples.
[a] Significant difference: $P < 0.05$.

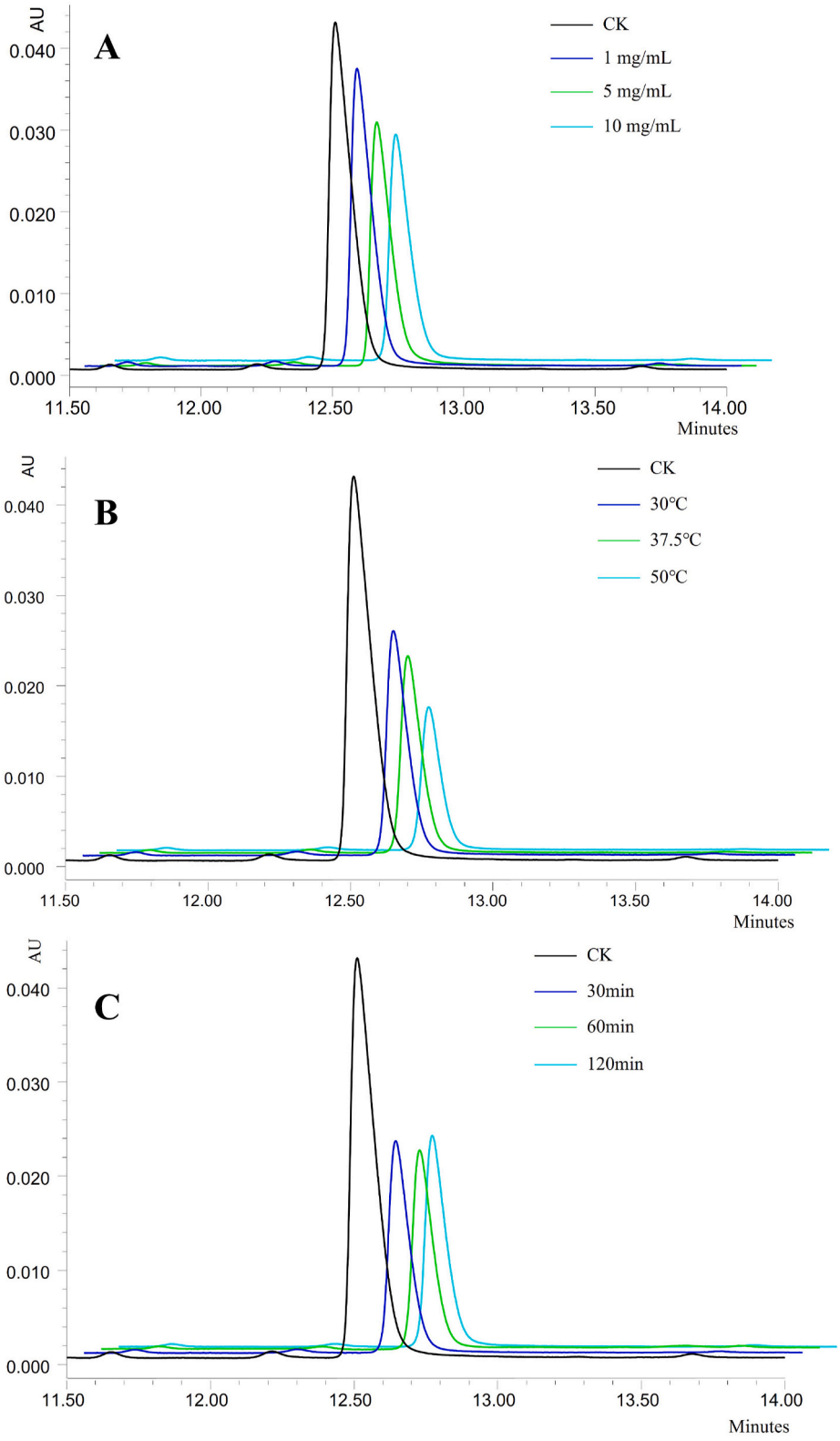

Fig. 1. The influence of different enzyme concentration (a), different temperature (b), and culture time (c) on the reaction.

the target protein to form combined complexes; and second, protein-ligands complexes were separated through the UF unit and the filtrates analyzed using UPLC [41]. Furthermore, a competitive group was additionally designed to distinguish selective binders from non-selective ligands as positive control group. HAase was pre-incubated with adequate DG to form the active-site-blocked HAase, which is less competitive to integrate with other potential ligands, then followed by incubation with the extract. The TIC peak areas were recorded, and BD/CBD values were calculated. The following criteria were applied to seek out presumptive compounds and minimize the false positive. Compounds with BD > 70% indicate their considerable binding affinity to the HAase, compounds with CBD >30% represent conspicuous advantage to the binding ability of DG to HAase. There were 19 components separated and detected from CME using LC-MS (Fig. 3A). Following the evaluation criteria mentioned above, eight potential candidate ligands in the UF chromatogram (**9**, **10**, **11**, **13**, **15**, **17**, **20,** and **21**) were observed by comparison with blank experiment (Fig. 3A and B), and four of them (**9**, **10**, **17,** and **21**) were distinguished with high BD values (86.72, 95.35, 96.98 and 98.01, respectively) (Fig. 3C and Table 3). Extracted ion chromatography (EIC) of screened compounds (**9**, **10**, **11**, **13**, **15**, **17**, **20**, and **21**) from CME are shown as Fig. 4. In addition, compounds **9**, **10**, **17,** and **21** were all considered as potent HAase specific inhibitor candidates as their CBD values were >30% (Table 3).

3.4. Identification of the screened ligands from CME

Structural identification of major HAase inhibitors was performed by matching their retention times, precursor ions, and characteristic fragment ions with reference standards and reported literatures. In this study, the Q-TOF-MS analysis of the compounds from CME was performed in negative ion mode. Three caffeoylquinic acid compounds (**13**, **15,** and **20**) exhibited the same deprotonated peaks ($C_{25}H_{23}O_{12}$, [M − H]-) at *m/z* 515, and the fragments were recorded at *m/z* 353, 191, and 135. Integrating the above information of ultraviolet (UV) spectra, mass spectrometry, and previous literature reports [12,34], compounds **13**, **15,** and **20** were tentatively identified as 1,4-*O*-Dicaffeoylquinic acid, 3,4-*O*-Dicaffeoylquinic acid and 4,5-*O*-Dicaffeoylquinic acid, respectively, which were validated using authentic reference standards. Compounds **9**, **10**, **11**, **17,** and **21** were identified as flavonoids, as associated with their flavonol characteristic in the UV spectrum. Compounds **10** and **11** showed deprotonated peaks ($C_{21}H_{19}O_{11}$, [M − H]-) at *m/z* 447 and peak ($C_{21}H_{17}O_{12}$, [M − H]-) at *m/z* 461, and the fragments at *m/z* 285, 151 suggested the same aglycone; the neutral loss of 162 and 176 mass units suggested the presence of glucoside and glucuronide, respectively (Fig. 5b). Therefore, compounds **10** and **11** were unambiguously assigned as luteoloside and luteolin-7-*O*-glucuronide, respectively, based on a previous report [12]. Similarly, by comparing the deprotonated peaks and characteristic fragments with previous reports [12,42], compounds **9**, **17,** and **21** were identified as eriodictyol-7-*O*-glucoside, apigenin-7-*O*-glucoside and diosmetin-7-*O*-glucoside, respectively (Fig. 5a, c, and 5d). The identity of these five flavonoids were all validated using authentic reference standards. All detailed data of these screened compounds are summarized in Table 3.

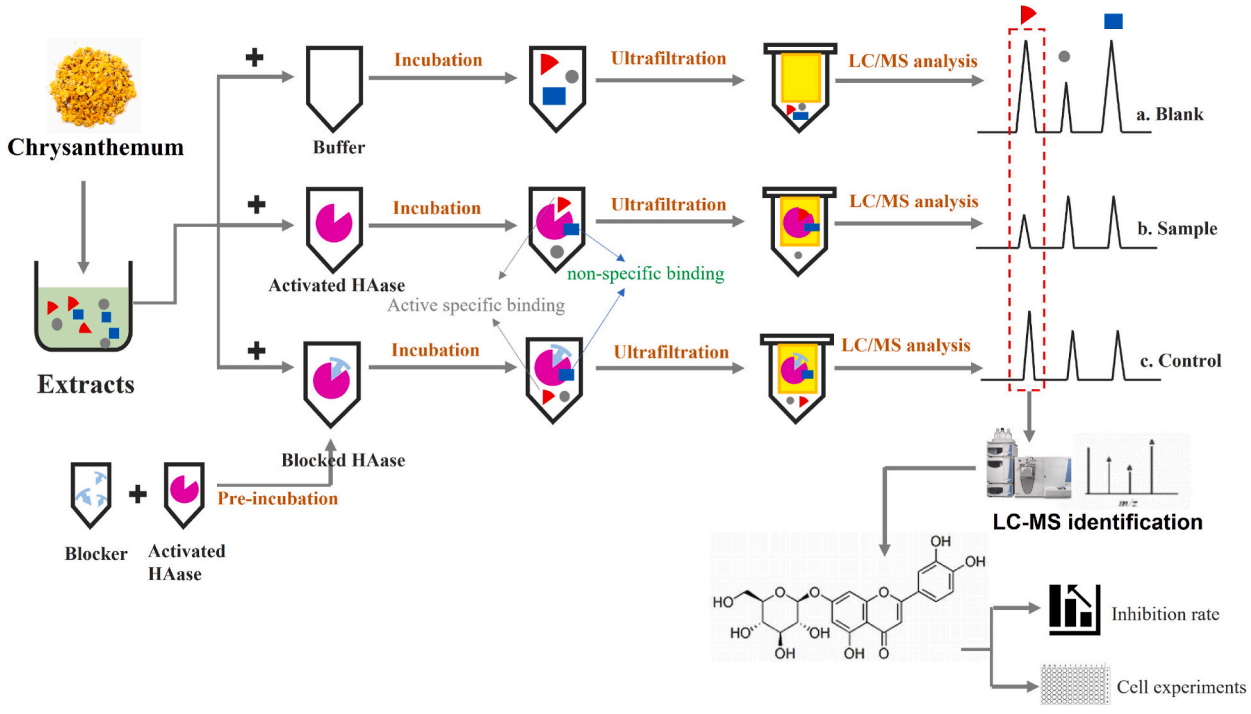

Fig. 2. Scheme of UF-UPLC-PDA-MS assay for screening for HAase inhibitors.

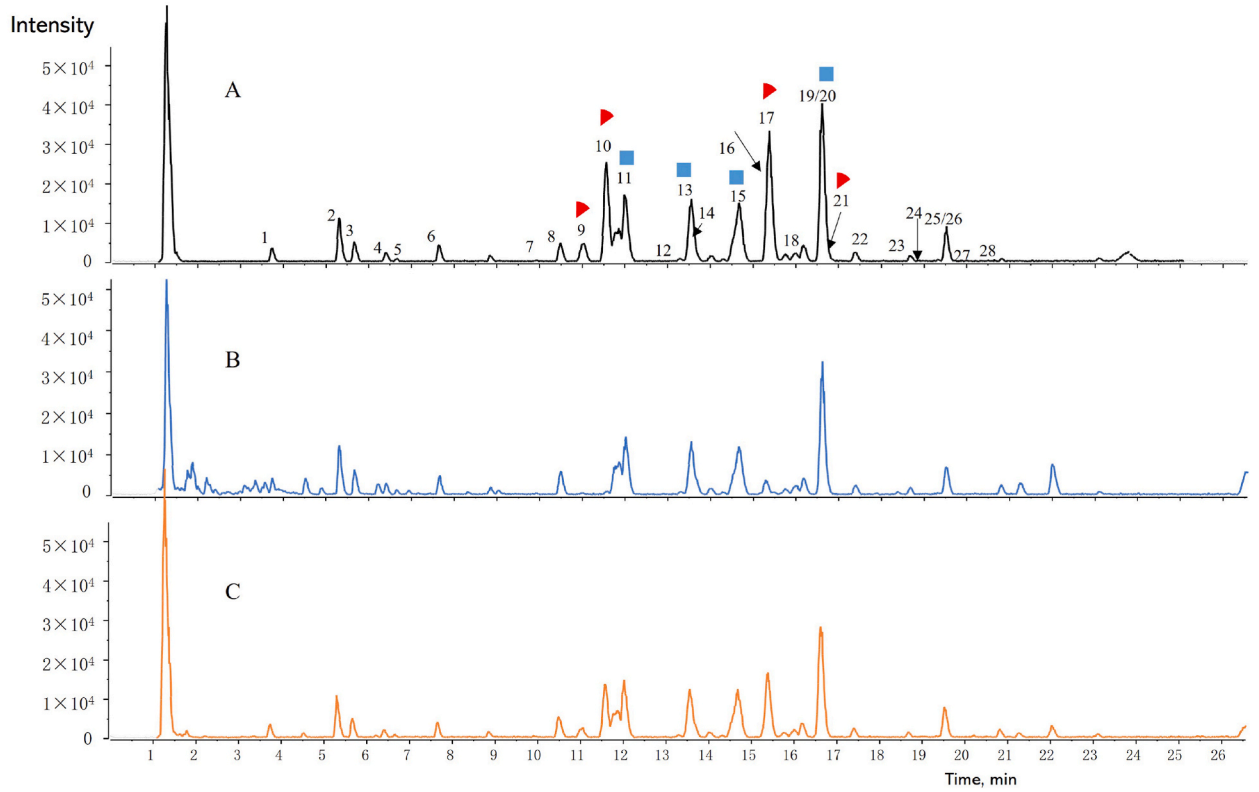

Fig. 3. UF-UPLC-MS analysis of CME for identifying the ligands bound to HAase. A. Chromatogram of the blank group. B. Chromatogram of the sample group. C. Chromatogram of the DG-blocked HAase group.

Table 3
Retention times (tR), MS data for identification of HAase inhibitors in CME using QTOF MS and Effect of candidate inhibitors on BD% and CBD%.

No.	TR (min)	Name	Molecular formula	M/Z [M − H]	MS/MS spectra	BD (%)	CBD (%)
9	11.02	Eriodictyol-7-O-glucoside	C21H22O11	449.1087	287.0553; 197.8070; 151.0034; 135.0451; 61.9890	86.72	41.59
10	11.56	Luteoloside	C21H20O11	447.0933	285.0397; 197.8072; 151.0093; 61.9884	95.35	51.86
11	12.01	Luteolin-7-O-glucuronide	C21H18O12	461.0721	285.0387; 197.0379; 61.9889	19.97	1.99
13	13.55	3,4-dicaffeoylquinic acid	C25H24O12	515.1216	353.0884; 191.0562; 135.0458; 61.9885	20.81	−1.07
15	14.67	3,5-dicaffeoylquinic acid	C25H24O12	515.1193	353.0852; 191.0553; 179.0337; 135.0452; 61.9885	19.38	−0.90
17	15.38	Apigenin 7-O-glucoside	C21H20O10	431.1009	431.0984; 268.0371	96.98	47.63
20	16.62	4,5-dicaffeoylquinic acid	C25H24O12	515.1209	353.0862; 191.0557; 179.0345; 135.0447	23.44	−1.08
21	16.85	Diosmetin 7-O-glucoside[a]	C22H22O11	507.1168	461.1024; 299.0543; 284.0290; 197.8080; 61.9883	98.01	59.14

[a] [M + FA-H].

3.5. Validation of the screened compounds on HAase inhibitory activities

Inhibitory effects of several isolated compounds from CME on HAase are shown in Table 4. The HAase inhibitory activities of compounds **9** and **21** were first reported in the present study. Among all tested compounds at a concentration of 1000 μM, only eriodictyol-7-O-glucoside (9), luteoloside (10), Luteolin-7-O-glucuronide (11), apigenin 7-O-glucoside (17), and diosmetin 7-O-glucoside (21) showed 40.15, 44.85, 13.72, 18.04, and 24.15% inhibition of HAase, respectively, with significant difference ($P < 0.05$) and 32.00% inhibition rate of DG as a positive control. At a concentration of 500 μM, only eriodictyol-7-O-glucoside (9) and luteoloside (10) displayed inhibitory activities on HAase with significant difference ($P < 0.05$) with values of 39.94 and 24.19%, respectively.

DG, a competitive inhibitor, was used as a HAase blocker and it preoccupied HAase specific site to prevent the binding of other potential ligands to the enzyme. Overall, only specific ligands should theoretically be distinguished as potential candidates theoretically. Our results from UF-UPLC-MS screening showed compounds **9**, **10**, **17**, and **21** as specific ligands, and compounds **11**, **13**, **15**,

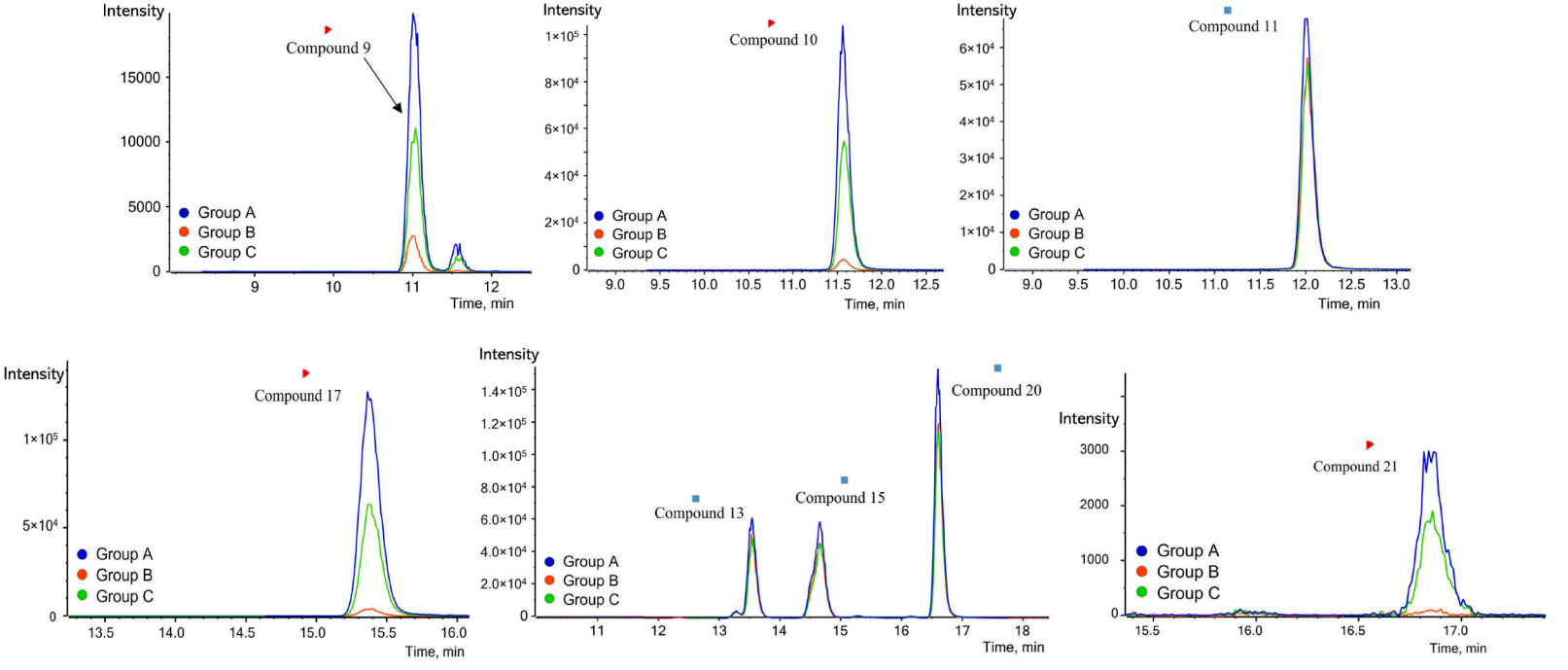

Fig. 4. EIC of screened compounds (**9**, **10**, **11**, **13**, **15**, **17**, **20**, and **21**) from CME for identifying the ligands bound to HAase. Group A. EIC of the blank group; Group B. EIC of the sample group; Group C. EIC of the DG-blocked HAase group.

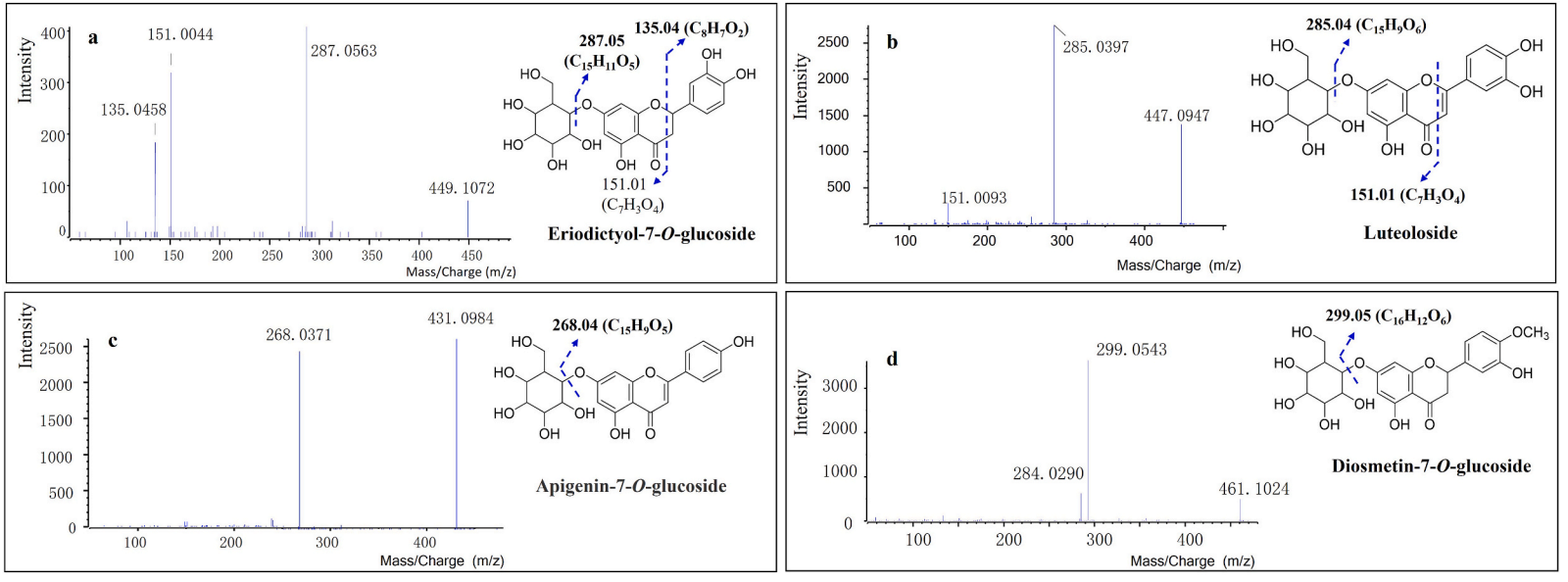

Fig. 5. Chemical structure and fragmentation pathway of (a) eriodictyol-7-*O*-glucoside, (b) luteoloside , (c) apigenin-7-*O*-glucoside, and (d) diosmetin 7-*O*-glucoside.

Table 4
Inhibitory effects of compounds on HAase activity.

HAase inhibition (% control)			
NO.	Compound	500 μM	1000 μM
9	Eriodictyol-7-O-glucoside	39.94 ± 9.03[a]	40.15 ± 7.49[a]
10	Luteoloside	24.19 ± 4.82[a]	44.85 ± 7.66[a]
11	Luteolin-7-O-glucuronide	3.87 ± 3.67	13.72 ± 4.37[a]
13	3,4-dicaffeoylquinic acid	−1.41 ± 1.77	6.65 ± 5.00
15	3,5-dicaffeoylquinic acid	5.20 ± 0.76	8.23 ± 4.33
17	Apigenin 7-O-glucoside	6.61 ± 3.92	18.04 ± 8.01[a]
20	4,5-dicaffeoylquinic acid	−0.96 ± 3.08	4.99 ± 2.46
21	Diosmetin 7-O-glucoside	7.40 ± 5.01	24.15 ± 6.57[a]
control	Dipotassium glycyrrhizate	29.92 ± 1.64[a]	32.00 ± 3.03[a]

All data were expressed as mean ± SD and the negative control value was approximately 0% inhibition of HAase without samples.
[a] Significant difference: $P < 0.05$.

and **20** as no-specific ligands. However, as a no-specific ligand, luteolin-7-*O*-glucuronide (**11**) still inhibited HAase activity at high concentration. The possible explanation was that although some compounds bind preferably to other non-specific sites instead of the active site or just have different binding sites as opposed to DG, it still influenced the configuration of active site to some extent, and thus showed some inhibitory capability. Possibly, false positives as well as the ligands that have different enzyme-binding sites with selected blocker will be eliminated in the process [27,43]. In general, luteolin-7-*O*-glucuronide (**11**) seemed to have a lower inhibitory activity against HAase compared to the other four specific compounds. Previously, some compounds, such as chlorogenic acid, were demonstrated to have no and weak HAase inhibitory activities which is similar to our current observations [44,45].

The traditional HAase inhibition method was complicated and required the use of a strong acid and alkali, which greatly affected UV absorption of flavonoid compounds, and large deviation was observed. In contrast, the binding ability evaluated using the UF-LC-MS method is relatively more stable and the process is simpler. Although the binding ability is not simply equal to the inhibitory effect, it may still be notably useful to identify potential HAase inhibitors.

3.6. Effects of the four compounds on NO release, pro-inflammatory cytokines, and relating gene expression

Several studies have shown that various flavonoids with strong inhibitory effects on HAase also have significant anti-inflammatory effects on in vitro cellular systems, such as the suppression of pro-inflammatory cytokine expression [46]. To fully understand and further confirm inflammatory properties of the four specific compounds, a LPS-induced cell inflammatory model in RAW264.7 and THP1 cells was used to detect their effects on inflammatory mediators and relevant gene expressions.

After preliminarily determining the cytotoxicity of different concentrations of the four compounds (Supplementary Materials), further cytotoxicity testing with different concentrations of the compounds against RAW 264.7 and THP1 cells in the presence of 50 ng/mL LPS was performed using the MTT assay (Supplementary Materials). Cytotoxic effects of 50 ng/mL LPS with the compounds were not observed on the two cell lines at the concentrations 3.125–50 μM, whereas only luteoloside was mildly toxic at 50 μM. Based on the above results, 50 ng/mL LPS with the concentrations 12.5–50 μM of the compounds were selected for the follow-up experiments.

The generation of NO synthesized by inducible NO synthase (iNOS) in various animal and human cells is a typical indication of inflammatory responses and is thought to be an indicative bi-marker to evaluate the response to inflammatory stimuli [47]. Inflammatory cytokines such as IL-6 and IL-1β have also been reported to be highly related with numerous inflammatory ailment [48].

As shown in Fig. 6A and B, LPS stimulation significantly increased the contents of NO and IL-6 in cultured human THP1 cells and mouse RAW264.7 cells. After treatment with the four compounds, the production of NO and IL-6 were significantly decreased by various degrees in a dose-dependent manner compared with that in the LPS-only group. Compared with control group, LPS treatment caused a major increase in mRNA expression of iNOS and IL-1β (Fig. 6C and D). All the four compounds significantly suppressed the mRNA level of IL-1β in a concentration-dependent manner (Fig. 6C) compared to those in the LPS-induced group. All four compounds also showed lower mRNA expression levels of iNOS in a dose-dependent manner (Fig. 6D) and the inhibition of NO production can be explained by the suppression of iNOS mRNA transcription (Fig. 6D). These results, to a certain degree, imply that all the four compounds effectively suppressed inflammation response in LPS-stimulated inflammatory macrophages. Collectively, these results suggest that the four screened compounds have significant anti-inflammatory that involves inhibiting HAase and suppressing pro-inflammatory cytokine and blocking related gene expression. These results further suggest that these four compounds may be useful for therapeutic management of inflammatory diseases.

4. Conclusions

In this study, a rapid and simple strategy based on UF-LC-MS was established for the discovery of selective HAase inhibitors from Flos *Chrysanthemum*. The method can bypass the conventional bioassay guided isolation and purification process and greatly accelerate the discovery of new specific active compounds from natural products. However, the major problem of the method is false positive results, which are caused by the non-specific binding of compounds to the inactive site of HAase. To address this concern, two assays

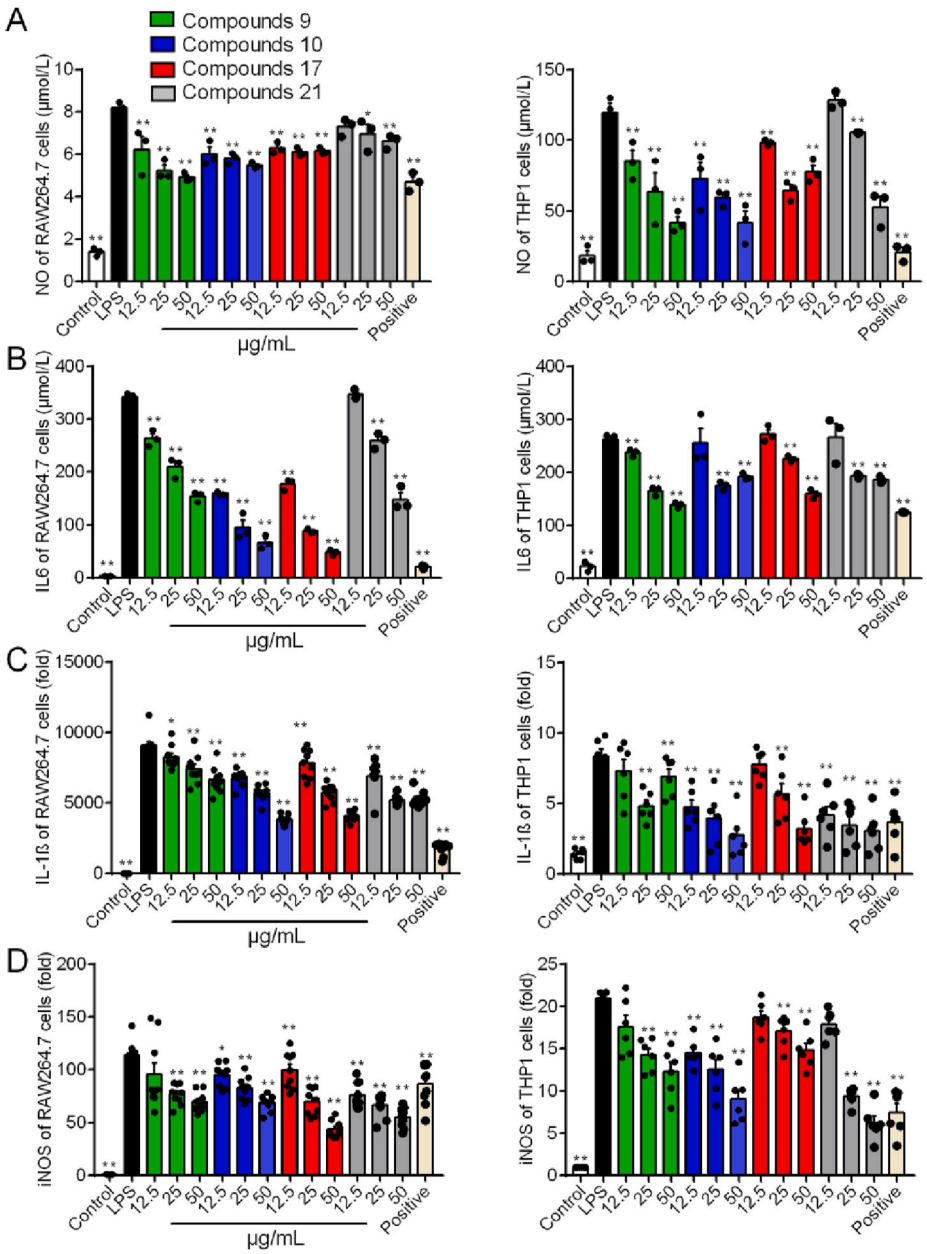

Fig. 6. Anti-inflammatory activity of four compounds in macrophages. The level of NO (A), IL-6 (B), TNF-α (C) was determined using an assay kit. The mRNA expressions of IL-1β (D), iNOS (E) and MyD88 (F) were measured by RT-qPCR. Values are presented as the x ± s, n = 3. Analyses were performed using a one-way ANOVA. ####$p < 0.001$ vs. the con group; *$p < 0.05$, **$p < 0.01$, ***$p < 0.001$, and ****$p < 0.0001$ vs. the LPS group. Compounds 9, 10, 17, and 21 were identified as eriodictyol-7-*O*-glucoside, luteoloside, apigenin 7-*O*-glucoside, and diosmetin 7-*O*-glucoside, respectively.

are typically applied. One routine solution is to compare the binding of compounds to the active and denatured enzyme to identify selective binders [49]. However, denatured HAase is insoluble, making this solution impractical. Another strategy is to introduce a competitive experiment by adding a known blocking agent to the incubation system, which possesses high affinity to the active site of the enzyme and blocks excessive binding of compounds to enzyme [50]. DG, a proven HAase blocker, was used as a competitive inhibitor to distinguish the selective ligands from the allosteric binders, which may minimize the occurrence of false positives. As a result, four specific ligands (eriodictyol-7-O-glucoside, luteoloside, apigenin-7-O-glucoside, and diosmetin 7-O-glucoside) and four no-specific ligands (luteolin-7-O-glucuronide, 1,4-O-Dicaffeoylquinic acid, 3,4-O-Dicaffeoylquinic acid and 4,5-O-Dicaffeoylquinic acid) from Flos *Chrysanthemum* were successfully screened and identified using this method. All four specific compounds significantly inhibited HAase activity at a concentration of 1000 μM. Although no-specific ligands, luteolin-7-*O*-glucuronide (11) have a

weaker inhibitory activity against HAase compared to the other four specific compounds relatively, it still displayed HAase inhibitory activity at 1000 μM. Possible explanation was that luteolin-7-*O*-glucuronide just have different binding sites as opposed to DG, but it still influenced the structure of active site to some extent, and thus showed some inhibitory capability.

The traditional HAase inhibition method was complicated and required the use of a strong acid and alkali, which greatly affected UV absorption of flavonoid compounds, and large deviation was observed. In contrast, the binding ability evaluated using UF-LC-MS is relatively more stable and the process is simpler. Because of the different binding mechanisms between varied enzymes and each compound, the highest affinity competitive inhibitors should be selected from known HAase inhibitors as the most suitable blockers. However, few stable positive drugs have been reported due to the complexity of HAase inhibition experiments. Accordingly, more stable positive HAase inhibitors can be compared in follow-up experiments in addition to DG. Although the binding ability is not simply equal to the inhibitory effect, it may still be useful in identifying potential HAase inhibitors.

In addition, our results indicate that the four screened flavonoids showed marked inhibition of the inflammatory mediator NO radicals, pro-inflammatory cytokine IL-6, and mRNA expression level of inflammatory genes such as iNOS and IL-1β as to relieve the symptoms of inflammatory responses. Collectively, these results suggest that the four screened compounds have significant anti-inflammatory activity that involves inhibiting HAase as well as suppressing pro-inflammatory cytokine and blocking related gene expression.

In conclusion, this study may facilitate the HAase inhibitors screening from complex mixtures and also provide more opportunities for the discovery and development of new therapeutic candidates from natural resources. In the future, animal tests and clinical trials of these compounds should be performed to further evaluate their bioavailability and anti-inflammatory activities.

Author contribution statement

Huiji Zhou: Conceived and designed the experiments; Performed the experiments; Analyzed and interpreted the data; Wrote the paper.Xue Zhang: Analyzed and interpreted the data.Bo Li: Contributed reagents, materials, analysis tools or data.Rongcai Yue: Conceived and designed the experiments; Analyzed and interpreted the data.

Funding statement

Rongcai Yue was supported by National Natural Science Foundation of China [82000554]; TCM Modernization Research, National Key R&D Program of China [2018YFC1706800]; Research Initiation Fund for High-level Talents of Fujian Medical University [XRCZX2018015].

Data availability statement

Data will be made available on request.

Declaration of competing interest

The authors declare that they have no known competing financial interests or personal relationships that could have appeared to influence the work reported in this paper.

Acknowledgments

N/A.

Appendix A. Supplementary data

Supplementary data to this article can be found online at https://doi.org/10.1016/j.heliyon.2023.e13709.

Abbreviations

CME	Chrysanthemum morifolium extract
UF-LC-MS	Ultrafiltration affinity liquid chromatography coupled with mass spectrometry
HAase	Hyaluronidase
DXM	Dexamethasone
DG	Dipotassium glycyrrhizinate
LPS	Lipopolysaccharides
DMSO	dimethyl sulfoxide
MTT	3-(4,5-dimethylthiazol-2-yl)-2,5-diphenyltetrazolium bromide

References

[1] A. Peng, et al., Classification of edible chrysanthemums based on phenolic profiles and mechanisms underlying the protective effects of characteristic phenolics on oxidatively damaged erythrocyte, Food Res. Int. 123 (2019) 64–74.
[2] L.-Z. Lin, J.M. Harnly, Identification of the phenolic components of chrysanthemum flower (Chrysanthemum morifolium Ramat), Food Chem. 120 (1) (2010) 319–326.
[3] Z. Zhang, et al., On-line screening of natural antioxidants and the antioxidant activity prediction for the extracts from flowers of Chrysanthemum morifolium ramat, J. Ethnopharmacol. 294 (2022), 115336.
[4] N. Zhang, et al., Insights into the importance of dietary chrysanthemum flower (Chrysanthemum morifolium cv. Hangju)-wolfberry (Lycium barbarum fruit) combination in antioxidant and anti-inflammatory properties, Food Res. Int. 116 (2019) 810–818.
[5] S. Wang, et al., *Study on the effects of sulfur fumigation on chemical constituents and antioxidant activity of Chrysanthemum morifolium cv. Hang-ju.* Phytomedicine 21 (5) (2014) 773–779.
[6] Q. Chu, et al., Determination and differentiation of Flos Chrysanthemum based on characteristic electrochemical profiles by capillary electrophoresis with electrochemical detection, J. Agric. Food Chem. 52 (26) (2004) 7828–7833.
[7] H. Yuan, et al., The flower head of Chrysanthemum morifolium Ramat. (Juhua): a paradigm of flowers serving as Chinese dietary herbal medicine, J. Ethnopharmacol. 261 (2020), 113043.
[8] Y. Li, et al., Chemical compositions of chrysanthemum teas and their anti-inflammatory and antioxidant properties, Food Chem. 286 (2019) 8–16.
[9] A.R. Han, et al., Phytochemical composition and antioxidant activities of two different color Chrysanthemum flower teas, Molecules 24 (2) (2019).
[10] G. Liu, et al., Protective effect of Chrysanthemum morifolium Ramat. ethanol extract on lipopolysaccharide induced acute lung injury in mice, BMC Complement Med Ther 20 (1) (2020) 235.
[11] Y.Y. Xie, et al., Comparative evaluation of cultivars of Chrysanthemum morifolium flowers by HPLC-DAD-ESI/MS analysis and antiallergic assay, J. Agric. Food Chem. 60 (51) (2012) 12574–12583.
[12] S. Chen, et al., Flavonoids and caffeoylquinic acids in Chrysanthemum morifolium Ramat flowers: a potentially rich source of bioactive compounds, Food Chem. 344 (2021), 128733.
[13] P.N. Sudha, M.H. Rose, Beneficial effects of hyaluronic acid, Adv. Food Nutr. Res. 72 (2014) 137–176.
[14] D. Jiang, J. Liang, P.W. Noble, Hyaluronan as an immune regulator in human diseases, Physiol. Rev. 91 (1) (2011) 221–264.
[15] C.C. Termeer, et al., Oligosaccharides of hyaluronan are potent activators of dendritic cells, J. Immunol. 165 (4) (2000) 1863–1870.
[16] G.C. Weber, et al., Clinical applications of hyaluronidase, Adv. Exp. Med. Biol. 1148 (2019) 255–277.
[17] B.A. Buhren, et al., Hyaluronidase: from clinical applications to molecular and cellular mechanisms, Eur. J. Med. Res. 21 (2016) 5.
[18] K.S. Girish, et al., Hyaluronidase inhibitors: a biological and therapeutic perspective, Curr. Med. Chem. 16 (18) (2009) 2261–2288.
[19] T. Shibata, et al., Inhibitory activity of brown algal phlorotannins against hyaluronidase, Int. J. Food Sci. Technol. 37 (6) (2010) 703–709.
[20] L. Scotti, et al., Recent advancement in natural hyaluronidase inhibitors, Curr. Top. Med. Chem. 16 (23) (2016) 2525–2531.
[21] Y. Genc, et al., The inhibitory effects of isolated constituents from Plantago major subsp. major L. on collagenase, elastase and hyaluronidase enzymes: potential wound healer, Saudi Pharmaceut. J. 28 (1) (2020) 101–106.
[22] E.M. Mohamed, et al., Bioassay-guided isolation, metabolic profiling, and docking studies of hyaluronidase inhibitors from ravenala madagascariensis, Molecules 25 (7) (2020).
[23] L. Xie, et al., Rapid and comprehensive profiling of α-glucosidase inhibitors in Buddleja Flos by ultrafiltration HPLC–QTOF-MS/MS with diagnostic ions filtering strategy, Food Chem. 344 (2020), 128651.
[24] G. Chen, B.X. Huang, M. Guo, Current advances in screening for bioactive components from medicinal plants by affinity ultrafiltration mass spectrometry, Phytochem. Anal. 29 (4) (2018) 375–386.
[25] S.Q. Wu, et al., A fast and accurate method for the identification of peroxidase inhibitors from Radix Salvia Miltiorrhizae by on-flow biochemical assay coupled with LC/Q-TOF-MS: comparison with ultrafiltration-based affinity selection, Anal. Bioanal. Chem. 410 (18) (2018) 4311–4322.
[26] X. Chen, et al., Identification of inhibitors of the antibiotic-resistance target New Delhi metallo-β-lactamase 1 by both nanoelectrospray ionization mass spectrometry and ultrafiltration liquid chromatography/mass spectrometry approaches, Anal. Chem. 85 (16) (2013) 7957–7965.
[27] H.P. Song, et al., Screening for selective inhibitors of xanthine oxidase from Flos Chrysanthemum using ultrafiltration LC–MS combined with enzyme channel blocking, J. Chromatogr. B 961 (2014) 56–61.
[28] Z. Wang, , H.S., B. Huang, S.S. Lim, Identification of tyrosinase specific inhibitors from Xanthium strumarium fruit extract using ultrafiltration-high performance liquid chromatography, J. Chromatogr. B 1002 (2015) 319–328.
[29] Z. Wang, et al., Competitive binding experiments can reduce the false positive results of affinity-based ultrafiltration-HPLC: a case study for identification of potent xanthine oxidase inhibitors from Perilla frutescens extract, J. Chromatogr., B: Anal. Technol. Biomed. Life Sci. 1048 (2017) 30–37.
[30] H. Ito, et al., Antiallergic activities of rabdosiin and its related compounds: chemical and biochemical evaluations, Bioorg. Med. Chem. 6 (7) (1998) 1051–1056.
[31] A.C. Pessini, et al., A hyaluronidase from Tityus serrulatus scorpion venom: isolation, characterization and inhibition by flavonoids, Toxicon 39 (10) (2001) 1495–1504.
[32] J.R. Soberón, et al., Free radical scavenging activities and inhibition of inflammatory enzymes of phenolics isolated from Tripodanthus acutifolius, J. Ethnopharmacol. 130 (2) (2010) 329–333.
[33] S.S. Han, S.J. Hur, S.K. Lee, A comparison of antioxidative and anti-inflammatory activities of sword beans and soybeans fermented with Bacillus subtilis, Food Funct. 6 (8) (2015) 2736–2748.
[34] Y. Li, et al., Chemical compositions of chrysanthemum teas and their anti-inflammatory and antioxidant properties, Food Chem. 286 (2019) 8–16.
[35] G. Chen, M. Guo, Rapid screening for α-glucosidase inhibitors from gymnema sylvestre by affinity ultrafiltration-HPLC-MS, Front. Pharmacol. 8 (2017) 228.
[36] X. Dong, B. Wang, J. Cao, Ligand fishing based on bioaffinity ultrafiltration for screening, xanthine oxidase inhibitors from citrus plants 44 (7) (2021) 1353–1360.
[37] H. Zhong, et al., Exploring the potential of novel xanthine oxidase inhibitory peptide (ACECD) derived from Skipjack tuna hydrolysates using affinity-ultrafiltration coupled with HPLC-MALDI-TOF/TOF-MS, Food Chem. 347 (2021), 129068.
[38] L.C. W, Method for manufacturing the skin cosmetics using horse bean and golden larch extract, in: South Korea Patent, 2005.
[39] W. Panthavee, et al., Characterization of exopolysaccharides produced by thermophilic lactic acid bacteria isolated from tropical fruits of Thailand, Biol. Pharm. Bull. 40 (5) (2017) 621–629.
[40] H. Liu, et al., Enzyme-site blocking combined with optimization of molecular docking for efficient discovery of potential tyrosinase specific inhibitors from puerariae lobatae radix, Molecules 23 (10) (2018).
[41] J.Q. Zhao, et al., Isolation and identification of antioxidant and α-glucosidase inhibitory compounds from fruit juice of Nitraria tangutorum, Food Chem. 227 (2017) 93–101.
[42] B.M. Johnson, D. Nikolic, R.B. van Breemen, Applications of pulsed ultrafiltration-mass spectrometry, Mass Spectrom. Rev. 21 (2) (2002) 76–86.
[43] Z. Wang, et al., Identification of tyrosinase specific inhibitors from Xanthium strumarium fruit extract using ultrafiltration-high performance liquid chromatography, J. Chromatogr., B: Anal. Technol. Biomed. Life Sci. 1002 (2015) 319–328.
[44] C. Ao, et al., Isolation and identification of antioxidant and hyaluronidase inhibitory compounds from Ficus microcarpa L. fil. bark, J. Enzym. Inhib. Med. Chem. 25 (3) (2010) 406–413.
[45] Ö.B. Acıkara, et al., Inhibitory activity of Podospermum canum and its active components on collagenase, elastase and hyaluronidase enzymes, Bioorg. Chem. 93 (2019), 103330.
[46] J.H. Lee, G.H. Kim, Evaluation of antioxidant and inhibitory activities for different subclasses flavonoids on enzymes for rheumatoid arthritis, J. Food Sci. 75 (7) (2010) H212–H217.

[47] F. Abekura, et al., Esculentoside B inhibits inflammatory response through JNK and downstream NF-κB signaling pathway in LPS-triggered murine macrophage RAW 264.7 cells, Int. Immunopharm. 68 (2019) 156–163.
[48] R.B. Polidoro, et al., Overview: systemic inflammatory response derived from lung injury caused by SARS-CoV-2 infection explains severe outcomes in COVID-19, Front. Immunol. 11 (2020) 1626.
[49] Y. Hong, X. Liao, Z. Chen, Screening and characterization of potential α-glucosidase inhibitors from Cercis chinensis Bunge fruits using ultrafiltration coupled with HPLC-ESI-MS/MS, Food Chem. 372 (2022), 131316.
[50] H. Wei, et al., Pharmaceutical applications of affinity-ultrafiltration mass spectrometry: recent advances and future prospects, J. Pharmaceut. Biomed. Anal. 131 (2016) 444–453.